Available online at www.sciencedirect.com

ScienceDirect

Nuclear Physics B 913 (2016) 815–833

NUCLEAR PHYSICS B

www.elsevier.com/locate/nuclphysb

Descent Equation for superloop and cyclicity of OPE

A.V. Belitsky

Department of Physics, Arizona State University, Tempe, AZ 85287-1504, USA

Received 20 May 2016; received in revised form 19 September 2016; accepted 17 October 2016

Available online 24 October 2016

Editor: Stephan Stieberger

Abstract

We study the so-called Descent, or $\bar{Q}$, Equation for the null polygonal supersymmetric Wilson loop in the framework of the pentagon operator product expansion. To properly address this problem, one requires to restore the cyclicity of the loop broken by the choice of OPE channels. In the course of the study, we unravel a phenomenon of twist enhancement when passing to a cyclically shifted channel. Currently, we focus on the consistency of the all-order Descent Equation for the particular case relating the NMHV heptagon to MHV hexagon. We find that the equation establishes a relation between contributions of different twists and successfully verify it in perturbation theory making use of available bootstrap predictions for elementary pentagons.

1. Introduction

The superamplitude $\mathcal{A}_N$ in planar $\mathcal{N}=4$ superYang–Mills theory is known to be dual to the superWilson loop [1–6]

$$\mathcal{W}_N = \exp\left(ig \oint_{C_N} \mathbb{A} \right), \tag{1}$$

defined by a superconnection $\mathbb{A}$ residing on a piecewise light-like contour C_N in chiral superspace. The $\mathcal{W}_N$, being an off-shell correlator, provides a fully nonperturbative description of $\mathcal{A}_N$.

E-mail address: andrei.belitsky@asu.edu.

http://dx.doi.org/10.1016/j.nuclphysb.2016.10.011

What makes this correspondence even more powerful is that $\mathcal{W}_N$ can systematically be analyzed in the multi-collinear regimes, i.e., when certain adjacent links become parallel [7–10]. This expansion receives a rigorous nonperturbative reincarnation within the so-called pentagon operator product expansion (OPE) [11]. The power of the latter lies in the fact that all of its ingredients can be computed to all orders in 't Hooft coupling making use of the hidden integrablility of the theory [11–22]. In spite of the fact that there is a plethora of data on scattering amplitudes that heavily relies on ordinary and dual superconformal symmetries [23–26], the above formalism obscures the most basic symmetries such as supersymmetry, cyclicity etc.

The chiral nature of the superWilson loop representation itself, while preserves some tree-level dual symmetries, masks others and makes them coupling dependent in spite of the fact that there are no intrinsic short-distance anomalies associated with them.[1] One particular generator that received a close attention in this regard was the Poincaré supersymmetry $\bar{Q}$ [26,27], i.e., the chiral conjugate of Q. Its action on the superloop was cast in an all-loop conjecture[2] [26] that was dubbed the Descent Equation, see Eq. (6) below. Its power was uncovered in the fact that it mixes different orders in perturbative series, enabling one to predict higher loop amplitudes from the ones an order lower. Of particular importance for this application was the cyclicity of the loop that provided contributions adding up together to yield correct final answer. As a consequence, the goal of the current study will be twofold. We will unravel how the cyclic permutations are implemented in the Descent Equation from the point of view of OPE. And then we will realize what the Descent Equation implies for the mixing of different twists in the operator series.

Our subsequent presentation is organized as follows. In the following section, we recap the form of the equation for the finite Wilson loop observables which are natural from the point of view of the pentagon OPE. Next, we provide a preliminary discussion of the Descent Equation by relating one-loop NMHV heptagon to two-loop MHV hexagon at leading twist in flux-tube excitations. As we observe there, to properly incorporate cyclic contributions we have, in principle, to resum the entire OPE series. To guide ourselves in the quest of uncovering cyclicity, we use available exact one-loop expressions for the heptagon and conjecture their form in terms of the OPE data to all orders in 't Hooft coupling. To confirm our prediction, we initiate a thorough OPE analysis of the NMHV heptagon by going beyond leading twist in Section 3. Then in Section 4, we verify, making use of our all-order predictions in 't Hooft coupling, that our hypothesis is indeed correct by going to one loop order higher when all genuine two-particle states start to contribute. Finally we conclude.

2. Collinear limit and Descent Equation

A natural observable from the point of view of the OPE is a properly subtracted superWilson loop $\mathcal{W}_N$. It is related to the ratio function $\mathcal{R}_N = \mathcal{A}_N/A_N^{\rm BDS}$ that was devised in Ref. [26] according to

$$\mathcal{W}_N = \mathcal{R}_N W_N^{\rm U(1)}\,. \tag{2}$$

[1] Of course, there are generators that do develop true anomalies due to ultraviolet divergencies, like conformal boost etc.

[2] To date, the Descent Equation viewed as a Ward identity of the antichiral supersymmetry generator has evaded rigorous studies due to lack of a proper regularization scheme that leaves manifest symmetries of the superloop intact. The main culprit in these analyses is the correlation functions of field equations of motion with superholonomies and strong UV divergencies associated with the light-cone nature of the contour [6].

Here $\ln W_N^{\mathrm{U}(1)}$ is the sum of connected correlators of the Wilson loops in U(1) theory between reference squares in a chosen tessellation of the N-gon with the coupling constant $g^2_{\mathrm{U}(1)}$ replaced by (one quarter of) the exact cusp anomalous dimensions in $\mathcal{N}=4$ theory, $\Gamma(g)=4g^2-8g^4\zeta_2+\dots$,

$$\ln W_N^{\mathrm{U}(1)}=\frac{1}{4}\Gamma(g)X\,. \tag{3}$$

The function X depends on $3N-5$ conformal cross ratios $X=X(u_1,\dots,u_{3N-5})$. The superloop admits a terminating expansion in Grassmann variables χ,

$$\mathcal{W}_N=\sum_{n=0}^{N-4}\mathcal{W}_{N,n}\,, \tag{4}$$

with each term being a degree-$4n$ polynomial in χ. They correspond to N^{n}MHV amplitudes, up to an overall factor of the 't Hooft coupling, namely, $\mathcal{W}_{N,n}=g^{2n}\mathcal{A}_{N,n}$.

The action of the $\bar{Q}$-operator,

$$\bar{Q}_\alpha^A=\sum_{i=1}^{N}\chi_i^A\frac{\partial}{\partial Z_i^\alpha}\,, \tag{5}$$

on the N-point N^{n}MHV observable can be cast in the form

$$\bar{Q}_\alpha^A\mathcal{W}_{N,n}=\frac{\Gamma(g)}{4g^2}\sum_{i=1}^{N+1}\int d^{2|3}\mathcal{Z}_{\alpha\,i}^A\left[\mathcal{W}_{N+1,n+1}-\mathcal{W}_{N+1,1}^{\mathrm{tree}}\mathcal{W}_{N,n}\right], \tag{6}$$

where in the right-hand side one takes a collinear limit of the $N+1$ point N^{n+1}MHV Wilson loop. Notice an extra factor of $1/g^2$ in the above equation that arises due to the aforementioned conversion from amplitudes to Wilson loops. The limit is accomplished by means of a proper parametrization of the near-collinear expansion of adjacent sites parametrized by supertwistors $\mathcal{Z}_i=(Z_i,\chi_i)$ built from momentum twistors Z_i [28] and their Grassmann counterparts χ_i. A particularly convenient form is gained in the OPE framework by encoding all inequivalent polygons with the action of symmetries of intermediate squares, see Appendix A. For the case at hand, the supersymmetric collinear limit emerges from the relation

$$\begin{aligned}\mathcal{Z}_1^{(N+1)}=\mathcal{Z}_{N+1}^{(N+1)}&-\mathrm{e}^{-\tau'}\mathcal{Z}_N^{(N+1)}+\mathrm{e}^{-\tau'+2\sigma'}(1+\mathrm{e}^{-\tau'-\sigma'+i\phi'})\mathcal{Z}_2^{(N+1)}\\&+\mathrm{e}^{-2\tau'+\sigma'+i\phi'}\mathcal{Z}_3^{(N+1)}\,,\end{aligned} \tag{7}$$

and subsequently taking $\tau'\to\infty$. This implies an expansion at the bottom of the polygon in terms of flux-tube excitations of increasing twist. The measure $d^{2|3}\mathcal{Z}_1$ [26], however,

$$d^{2|3}\mathcal{Z}_{\alpha\,1}^A=\oint\limits_{|\varepsilon|=0_+}\frac{d\varepsilon'\varepsilon'}{2\pi i}\int d\mathrm{e}^{2\sigma'}\int(d^3\chi_1)^A\,\bar{n}_\alpha\,, \tag{8}$$

— where we defined $\varepsilon'=\mathrm{e}^{-\tau'}$ and $\bar{n}_\alpha=\varepsilon_{\alpha\beta\gamma\delta}Z_{n-1}^\beta Z_n^\gamma Z_1^\delta$, — singles out just one flux-tube fermion.

2.1. Preliminaries on Descent Equation

The right-hand side of the Descent Equation projects out a single fermionic excitation on the bottom of the polygon, while the top can absorb any multi-particle states with overall fermionic quantum numbers. Let us, however, start our analysis by considering its left-hand side. We will focus on the MHV hexagon as a case of study. At leading twist, it receives a contribution from a single gauge field created from the vacuum in the operator channel chosen by the parametrization of the momentum twistors introduced in the Appendix A,

$$\mathcal{W}_{6,0} = 1 + (\mathrm{e}^{i\phi} + \mathrm{e}^{-i\phi})\mathrm{e}^{-\tau}\mathcal{W}_{6[1](2)} + \dots , \tag{9}$$

with[3] [16]

$$\mathcal{W}_{6[1](2)} = \int_{\mathbb{R}} d\mu_{\mathrm{g}}(v) . \tag{10}$$

Here we used a compound notation for the differential measure of the p-type flux-tube excitation along with the propagating phase encoded by its energy E_{p} and momentum p_{p},

$$d\mu_{\mathrm{p}}(v) = \frac{dv}{2\pi}\mu_{\mathrm{p}}(v)\mathrm{e}^{-\tau[E_{\mathrm{p}}(v)-1]+i\sigma p_{\mathrm{p}}(v)} \tag{11}$$

For brevity, we select $\alpha = 4$ component of the $\bar{Q}^A_\alpha$ generator. Its action can be easily evaluated on the twist-one hexagon to read

$$\bar{Q}^A_4\mathrm{e}^{-\tau}\mathcal{W}_{6[1](2)} = \chi^A_4\mathrm{e}^{-\tau}\int_{\mathbb{R}} d\mu_{\mathrm{g}}(v)\tfrac{1}{2}\big(E_{\mathrm{g}}(v) + ip_{\mathrm{g}}(v)\big) + \dots , \tag{12}$$

where ellipses stand for cyclic contributions accompanied by other Grassmann variables. Expanding the measure, $\mu_{\mathrm{p}} = g^2\mu^{(1)}_{\mathrm{p}} + g^4\mu^{(2)}_{\mathrm{p}} + \dots$, the energy and momentum, $E_{\mathrm{p}} = 1 + g^2E^{(1)}_{\mathrm{p}} + \dots$ and $p_{\mathrm{p}} = 2u + g^2p^{(1)}_{\mathrm{p}} + \dots$ in perturbative series, we can shift the integration contour into the lower half of the complex rapidity plane, $v \to v - \frac{i}{2}$ and rewrite the result in the form

$$\begin{aligned}\bar{Q}^A_4\mathrm{e}^{-\tau}\mathcal{W}_{6[1](2)} = \chi^A_4\mathrm{e}^{-\tau}\int_{\mathbb{R}+i0}\frac{dv}{2\pi}\mathrm{e}^{2iv\sigma}\Big\{&g^2\mathrm{e}^{\sigma}\mu^{(1)}_{\mathrm{F}}(v)\\ &+ g^4\Big[\mathrm{e}^{\sigma}\Big(\mu^{(2)}_{\mathrm{F}}(v) + (i\sigma p^{(1)}_{\mathrm{F}}(v) - \tau E^{(1)}_{\mathrm{F}}(v))\mu^{(1)}_{\mathrm{F}}(v)\Big)\\ &- \Big(2\tau + 2\sigma - ip^{(1)}_{\mathrm{g}}(v)\Big)\mu^{(1)}_{\mathrm{g}}(v)\Big] + O(g^6)\Big\} + \dots ,\end{aligned} \tag{13}$$

at the lowest two orders of perturbation theory. To arrive at this expression we used the following results. First, it is immediate to demonstrate that[4]

$$E_{\mathrm{g}}(v - \tfrac{i}{2}) = E_{\mathrm{F}}(v) - ip_{\mathrm{f}}(v - i) , \qquad p_{\mathrm{g}}(v - \tfrac{i}{2}) = p_{\mathrm{F}}(v) - iE_{\mathrm{f}}(v - i) , \tag{14}$$

[3] Here and below, we accept a notation that the subscripts in $\mathcal{W}_{N[t_1,\dots,t_{3N-5}](h_1,\dots,h_{3N-5})}$ stand for the number of cusps in the superloop N, with twists $t_1, \dots$ of excitations propagating on sequential intermediate squares and their corresponding total double helicities being $h_1, \dots$.

[4] Cf. these to the relations $E_{\mathrm{F}}(v) - E_{\mathrm{h}}(v - \frac{i}{2}) = ip_{\mathrm{f}}(v)$ and $p_{\mathrm{F}}(v) - p_{\mathrm{h}}(v - \frac{i}{2}) = iE_{\mathrm{f}}(v)$ found in Ref. [13].

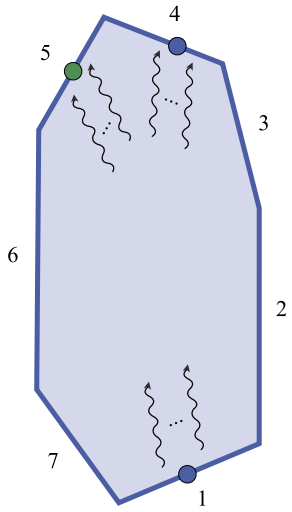

Fig. 1. Two OPE channels relevant for the Descent Equation involving heptagon. The two channels are obtained from each other by a mirror reflection with respect to the line going through Z_1 and connecting to the vertex $Z_4 \wedge Z_5$.

by confirming these identities order-by-order in 't Hooft coupling. For the measures, we have in the lowest few orders

$$(i-v)\mu_{\rm g}^{(1)}(v-\tfrac{i}{2}) = i\mu_{\rm F}^{(1)}(v)\,,$$
$$(i-v)\mu_{\rm g}^{(2)}(v-\tfrac{i}{2}) = i\mu_{\rm F}^{(2)}(v) - \tfrac{i}{2}E_{\rm g}^{(1)}(v-\tfrac{i}{2})\mu_{\rm g}^{(1)}(v-\tfrac{i}{2}) + \frac{\pi(1+2iv)}{v^2(v-i)^2\sinh(\pi v)}\,.$$

A naked eye inspection of Eq. (13) then immediately suggests that the first line and the first term in the second line emerge from a single-fermion exchange, as anticipated from the Descent Equation. This can easily be verified by computing the σ' integral of the $\chi_1^3\chi_4$ component (26) of the heptagon, see Fig. 1, which is extracted by the $d^{2|3}\mathcal{Z}_1$ measure. It yields to the lowest two orders in g^2

$$\int d\sigma'\,\mathcal{W}^{(4)}_{7[1,1](1,1)}(\sigma',\sigma) = -{\rm e}^{\sigma}\int\frac{dv}{2\pi}{\rm e}^{2iv\sigma}\Big\{g^2\mu_{\rm F}^{(1)}(v) + g^4\Big[\mu_{\rm F}^{(2)}(v) + (i\sigma p_{\rm F}^{(1)}(v) - \tau E_{\rm F}^{(1)}(v) + 2\zeta_2)\mu_{\rm F}^{(1)}(v)\Big] + O(g^6)\Big\}\,. \tag{15}$$

The ζ_2 term gets canceled upon multiplication by the cusp anomalous dimension thus providing agreement alluded to above. However, the second term in the square brackets of Eq. (13) is much more enigmatic. Since we currently lack understanding of the mechanism responsible for its emergence from the point of view of the underlying flux-tube dynamics, we will choose a more pragmatic route in the next section.

2.2. *Hints from one-loop analysis: the conjecture*

As a guide on our quest to unravel the aforementioned "problematic" contribution, we will start with an exact expression for the one-loop NMHV heptagon to see what we should anticipate

as its origin. In fact, the collinear limit of the heptagon ($N = 7$) was worked out in Ref. [26] for the ratio function $\mathcal{P}_N$ defined as

$$\mathcal{W}_N = \mathcal{P}_N \mathcal{W}_{N,0}\,, \tag{16}$$

with $\mathcal{W}_{N,0}$ being the bosonic, i.e., the lowest Grassmann, component of the superloop. $\mathcal{P}_N$ admits the same decomposition in the fermionic variables χ as $\mathcal{W}_N$ in Eq. (4) with $\mathcal{P}_{N,0} = 1$. From the point of view of the OPE, $\mathcal{W}_N$ and $\mathcal{P}_N$ coincide at one-particle level, but they start to deviate at two and beyond due to subtraction terms in $\mathcal{P}_N$, see, e.g., Eq. (43) below. Its degree $4n$ Grassmann component is naturally defined in terms of the ratio

$$\mathcal{P}_{N,n} = \mathcal{A}_{N,n}/\mathcal{A}_{N,0} \tag{17}$$

of the N^{n}MHV superamplitude $\mathcal{A}_{N,n}$ to the maximally helicity violating one $\mathcal{A}_{N,0}$.

According to [26], one finds

$$\begin{aligned}\int d^{2|3}\mathcal{Z}^A_{\alpha 1}\mathcal{P}_{7,1} =& \bar{Q}^A_\alpha \ln\frac{\langle 6724\rangle}{\langle 6723\rangle}\int_0^\infty dt\, I^{(4)}(t|w_1,w_2,w_3,w)\\ &+ \bar{Q}^A_\alpha \ln\frac{\langle 6725\rangle}{\langle 6723\rangle}\int_0^\infty dt\, I^{(5)}(t|w_1,w_2,w_3,w)\,,\end{aligned} \tag{18}$$

with the right-hand side being the function of cross ratios introduced in Appendix A. The two contributions can clearly be distinguished from one another by identifying them from the $\chi_1^3\chi_4$ and $\chi_1^3\chi_5$ Grassmann structures, in the first and second term, respectively. These correspond, in the OPE language, to a single fermion emitted at the bottom of the heptagon and all twists coupled to the top. However, the two are absorbed in adjacent OPE channels (see Fig. 1). The collinear expansion on the top of the heptagon admits a systematic classification within the pentagon framework, namely, we immediately find for the two contributions

$$\begin{aligned}\mathrm{e}^{2\sigma'} I^{(4)}(\mathrm{e}^{2\sigma'}|w_1,w_2,w_3,w) =& -\mathrm{e}^{-\tau}\mathcal{P}^{(4)}_{7\,[1,1](1,1)}(\sigma',\sigma,\tau'=0,\tau)\\ &-\mathrm{e}^{-2\tau}\left(\mathrm{e}^{i\phi}\mathcal{P}^{(4)}_{7\,[1,2](1,3)}+\mathrm{e}^{-i\phi}\mathcal{P}^{(4)}_{7\,[1,2](1,-1)}\right)\\ &\times(\sigma',\sigma,\tau'=0,\tau)+O(\mathrm{e}^{-3\tau})\,,\end{aligned} \tag{19}$$

$$\begin{aligned}\mathrm{e}^{2\sigma'} I^{(5)}(\mathrm{e}^{2\sigma'}|w_1,w_2,w_3,w) =& -\mathrm{e}^{-\tau}\mathcal{P}^{(5)}_{7\,[1,1](1,1)}(\sigma',\sigma,\tau'=0,\tau)\\ &-\mathrm{e}^{-2\tau}\left(\mathrm{e}^{i\phi}\mathcal{P}^{(5)}_{7\,[1,2](1,3)}+\mathrm{e}^{-i\phi}\mathcal{P}^{(5)}_{7\,[1,2](1,-1)}\right)\\ &\times(\sigma',\sigma,\tau'=0,\tau)+O(\mathrm{e}^{-3\tau})\,,\end{aligned} \tag{20}$$

which arise from the following generic form of the Grassmann expansion for $\mathcal{P}_{7,1}$

$$\mathcal{P}_{7,1} = \sum_{j=4,5}\chi_1^3\chi_j\sum_{n_1,n_2}\sum_{h_1,h_2}\mathrm{e}^{-n'\tau'-n\tau}\mathrm{e}^{i(h'\phi'+h\phi)/2}\mathcal{P}^{(j)}_{7[n',n](h',h)}(\sigma',\sigma,\tau',\tau;g)+\ldots\,. \tag{21}$$

The ellipses stand for irrelevant Grassmann structures and the nomenclature for the labels is the same as for $\mathcal{W}$ and was explained in the footnote 3. The remaining dependence of the ratio functions $\mathcal{P}^{(j)}_{7[n',n](h',h)}$ on the τ and τ' is polynomial in nature and comes from perturbative corrections to the eigen-energies of flux-tube excitations. Above, in Eqs. (19) and (20), we set τ'

to zero everywhere since these contributions vanish after σ' integration owing to the Goldstone theorem [30].

The proper reconstruction of the left-hand side of the Descent Equation requires adding up all cyclic permutation of Eq. (18) in the right-hand side of Eq. (6). Thus, the cyclic image of χ_5 will induce a contribution to the χ_4 structure after the shift $i \to i-1$. From the point of view of the all-twist function $I^{(5)}$, given by the expression [26],

$$
\begin{aligned}
I^{(5)}(t|w_1,w_2,w_3,w) = -\frac{w_3}{t(w_3+t)}\Bigg[&- \ln(1+t)\ln\frac{1+t}{t} \\
&- \ln\frac{w_3(1+t)}{w_3+t}\ln\frac{w_2(w_3+t)}{t} + \mathrm{Li}_2(1-w_2) + \mathrm{Li}_2(1-w_3) \\
&- \mathrm{Li}_2\left(\frac{1-w_3}{1+t}\right) + \mathrm{Li}_2\left(1-\frac{w_2}{1+t}\right)\Bigg] \\
&+ \frac{1}{t(w_3+t)}\Bigg[\ln\frac{w_3(w_3+t)}{w_3+t}\ln\frac{w_3+t}{t} + \mathrm{Li}_2(1-w_1) \\
&- \mathrm{Li}_2\left(1-\frac{w_1t_1}{w_3+t}\right)\Bigg] + \frac{w-w_3}{1+t}\Bigg[\ln\frac{w_2}{1+t}\ln\frac{w_1t}{w_3+t} \\
&+ \mathrm{Li}_2\left(1-\frac{w_2}{1+t}\right) + \mathrm{Li}_2\left(1-\frac{w_1t}{w_3+t}\right) - \zeta_2\Bigg]
\end{aligned}
\tag{22}
$$

this is achieved by a cyclic shift of twistors that results in a change of the cross ratios $w \to \tilde{w}$ as shown in Eqs. (64) of Appendix A. After this is done, we can safely expand the result in the collinear $\tau \to \infty$ limit to find its leading twist contribution in the χ_4 operator channel. While it is easy to find the functional from this Taylor expansion, to cast it back into the form of flux-tube integrand is extremely non-trivial.

Though it appears that one needs to restore the exact dependence on the cross ratios before moving to a different channel by resumming the entire OPE series, we found that one merely has to move beyond leading twist in the adjacent channel to induce a leading contribution after the cyclic shift. The result of our analysis is summarized by the following conjecture

$$
\begin{aligned}
&\int_{-\infty}^{\infty} d\sigma'\, \mathrm{e}^{2\sigma'} I_5(\mathrm{e}^{2\sigma'}|\tilde{w}_1,\tilde{w}_2,\tilde{w}_3,\tilde{w}) \\
&\quad = 0 - \mathrm{e}^{-\tau}\int_{-\infty}^{\infty} d\sigma'\Big[i\left(\mathcal{P}^{(5)}_{7\,[1,2](1,3)} - \mathcal{P}^{(5)}_{7\,[1,2](1,-1)}\right)\sin\phi \\
&\qquad + \left(\mathcal{P}^{(4)}_{7\,[1,2](1,-1)} + \mathcal{P}^{(4)}_{7\,[1,2](1,3)} - \mathcal{P}^{(5)}_{7\,[1,2](1,3)} - \mathcal{P}^{(5)}_{7\,[1,2](1,-1)} + \mathrm{e}^{\sigma}\mathcal{P}^{(4)}_{7\,[1,1](1,1)}\right)\cos\phi\Big] \\
&\qquad + O(\mathrm{e}^{-2\tau}),
\end{aligned}
\tag{23}
$$

for the integrand before the σ'-integration. Here the leading-twist effect in the χ_5 channel vanishes upon the integration! The subleading terms are expressed by means of twist-two contributions to the ratio functions for the χ_4 and χ_5 Grassmann components introduced earlier in Eq. (21). The helicity-preserving term, proportional to $\cos\phi$ and thus mimicking the azimuthal dependence of the leading twist gluon exchange (9), defines the leading effect in the χ_4-channel of the Descent Equation after the cyclic shift. This is the effect of twist enhancement we alluded

to in the Introduction. This expression can be cast in a very concise form at this order in 't Hooft coupling making use of the analysis that follows, namely,

$$2\int_{-\infty}^{\infty} d\sigma' \Big(\mathcal{P}^{(4)}_{7\,[1,2](1,-1)} + \mathcal{P}^{(4)}_{7\,[1,2](1,3)} - \mathcal{P}^{(5)}_{7\,[1,2](1,3)} - \mathcal{P}^{(5)}_{7\,[1,2](1,-1)} + \mathrm{e}^{\sigma}\mathcal{P}^{(4)}_{7\,[1,1](1,1)}\Big)$$
$$= -g^4 \int_{\mathbb{R}+i0} \frac{dv}{2\pi} \mathrm{e}^{2iv\sigma} \mu^{(1)}_{\mathrm{g}}(v) \Big(2\tau + 2\sigma - i p^{(1)}_{\mathrm{g}}(v)\Big) + O(g^6)\,. \tag{24}$$

As we can see, the $O(g^4)$ contribution is in agreement with the last term in Eq. (13).

At this point, the left-hand side of the above equation appears to be just one of may ways to reproduce the flux-tube integrand in the right-hand side and is merely a low-order coincidence. A priori, one does not even have a solid argument that such a representation is at all possible, except for an analogy with crossing a fermionic excitation from one OPE channel to another: a procedure that results in increasing its twist as well [17]. Therefore, to confirm this conjecture and put it on a firmer foundation, we would like to push on and set our goal at verifying it at higher perturbative orders. Thus, in the rest of the paper we will construct the OPE up to two particles on the top of the heptagon both in $\chi_1^3\chi_4$ and $\chi_1^3\chi_5$ channels. In this manner, we will have exact results for any value of the coupling constant and can confirm the validity of our hypothesis for the integrand in the left-hand side of Eq. (24).

3. Fermionic heptagon

As we stated above, we have to uncover the structure of subleading corrections in the OPE expansion of fermionic components of the heptagon superloop $\mathcal{W}_7$. Thus we turn to a thorough analysis of the $\chi_1^3\chi_4$ and $\chi_1^3\chi_5$ Grassmann structures with the emphasis on the lowest twist contribution at the bottom and up to twist two on the top. The general form of its Grassmann expansion is identical to Eq. (21) where we have to replace $\mathcal{P} \to \mathcal{W}$.

3.1. Twist-one: fermion exchange

To start with, we will recall the leading effect from the twist-one fermion propagating in the OPE channels in question [20], i.e., proportional to $\mathrm{e}^{-\tau'-\tau}\mathrm{e}^{i\phi'/2+i\phi/2}$. Both the $\chi_1^3\chi_4$ and $\chi_1^3\chi_5$ Grassmann structures are cumulatively given by

$$\mathcal{W}^{(j)}_{7[1,1](1,1)}(\sigma',\sigma) = \int_{\mathbb{C}^+_\Psi} d\mu_\Psi(u) x[u] \int_{\mathbb{C}^{(j)}_\Psi} d\mu_\Psi(v) P_{\Psi|\Psi}(-u|v)\,. \tag{25}$$

They are expressed in terms of the helicity non-flip fermionic pentagon transition $P_{\Psi|\Psi}$ [17] with the measure of the initial-state fermion accompanied by a helicity form factor given by the Zhukowski variable $x[u] = \frac{1}{2}(u + \sqrt{u^2 - (2g)^2})$. Above, the integration contours are shown in Fig. 2. The one for the fermion on the bottom of the heptagon is $\mathbb{C}^+_\Psi = \mathbb{C}^+_{\mathrm{F}} + \mathbb{C}^-_{\mathrm{f}}$ with $\mathbb{C}^+_{\mathrm{F}} = \mathbb{R} + i0$ and $\mathbb{C}^-_{\mathrm{f}}$ running a half-circle in the lower semiplane of the complex plane. The top contour depends on the supertwistor that the flux-tube excitation is "attached" to. For the $\chi_1^3\chi_4$ channel it is the same $\mathbb{C}^{(4)}_\Psi = \mathbb{C}^+_\Psi$, while for $\chi_1^3\chi_5$, it is "flipped" on the Riemann surface with respect to the imaginary axis, i.e., $\mathbb{C}^{(5)}_\Psi = \mathbb{C}^-_\Psi = \mathbb{C}^-_{\mathrm{F}} + \mathbb{C}^+_{\mathrm{f}}$. It can be explained by the fact that the latter

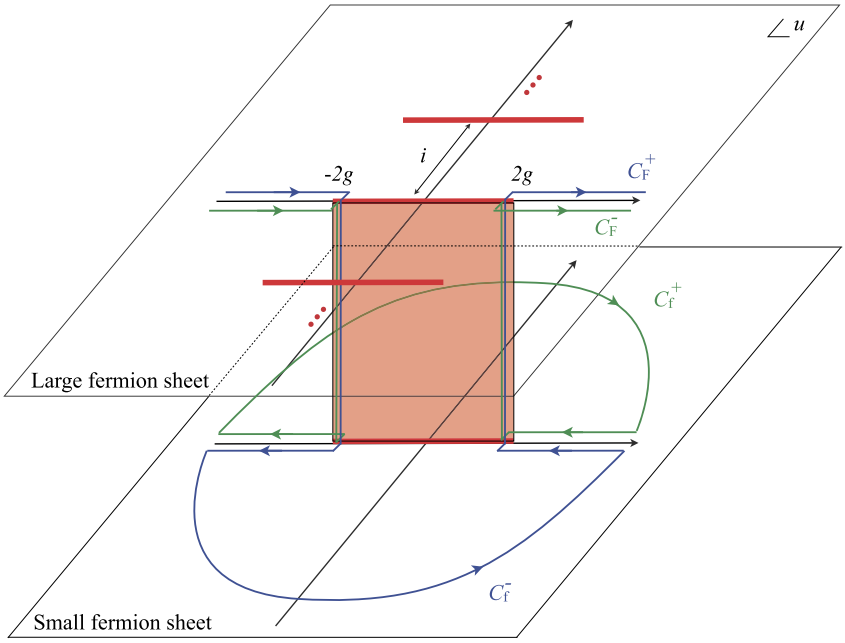

Fig. 2. The large and small fermion complex planes are glued together along the square root branch cut on the real axis $[-2g, 2g]$ (shown by the bold red interval) into a two-sheeted Riemann surface. The integration contours for the fermions in the OPE expressions are shown for the χ_4 in blue, $\mathbb{C}_\Psi^+ = \mathbb{C}_{\rm F}^+ + \mathbb{C}_{\rm f}^-$, and for χ_5 one in green, $\mathbb{C}_\Psi^- = \mathbb{C}_{\rm F}^- + \mathbb{C}_{\rm f}^+$, paths. (For interpretation of the references to color in this figure legend, the reader is referred to the web version of this article.)

channel is a mirror reflection of the original $\chi_1^3\chi_4$ one, thus in a given tessellation it corresponds to a different collinear limit.

In perturbation theory, as explained in Refs. [17,20], only the large fermion contributes to the OPE, yielding

$$\mathcal{W}^{(4,5)}_{7[1,1](1,1)}(\sigma',\sigma) = \int\limits_{\mathbb{R}+i0} d\mu_{\rm F}(u)x[u] \int\limits_{\mathbb{R}\pm i0} d\mu_{\rm F}(v)P_{\rm F|F}(-u|v)\,. \tag{26}$$

Its expansion in 't Hooft coupling can be easily verified to agree with explicit amplitudes by using, for instance, the package of Ref. [29]

The Descent Equation involves an integral over the position σ'. Our analysis reveals that the result is given by

$$\Gamma(g)\int d\sigma'\,\mathcal{W}^{(4)}_{7[1,1](1,1)}(\sigma',\sigma) = -2ig^2\int\limits_{\mathbb{R}+i0} d\mu_\Psi(v)\,, \tag{27}$$

where the prefactor of the exact cusp anomalous dimension arises from the integral

$$\int du\,\mu_\Psi(u)\mathrm{e}^{-\tau'[E_\Psi(u)-1]}x[u]\delta\big(p_\Psi(u)\big)P_{\Psi|\Psi}(-u|v) = -\frac{2ig^2}{\Gamma(g)}\,. \tag{28}$$

Superficially the left-hand side depends on the rapidity v, but in reality it is only a function of the 't Hooft coupling. Notice that the dependence on the cross-ratio τ' trivializes in light of the fact that the fermion mass is one at any value of the coupling [30],

$$p_\Psi(u) = 0\,, \qquad E_\Psi(u) = 1\,. \tag{29}$$

Equation (28) can be found by studying the fermion zero momentum limit which corresponds to the infinite rapidity on the small fermion Riemann sheet. It can be then checked by an explicit perturbative expansion to a very high order in 't Hooft coupling.

For the $\chi_1^3\chi_5$ channel, the fermion contour in the final state runs below the real axis. However, due to the Fourier exponent it has to be closed in the upper half plane. As a result, moving the contour just above the real axis, one picks up a pole at $v = 0$ on the real axis. The latter term induces a divergent contribution when integrated with respect to σ'. Namely, we find that it is coupling independent

$$\operatorname*{res}_{v=0} P_{\mathrm{F}|\mathrm{F}}(-u|v)\mu_{\mathrm{F}}(v)\mathrm{e}^{-\tau[E_{\mathrm{F}}(v)-1]+i\sigma p_{\mathrm{F}}(v)} = -i\,, \tag{30}$$

such that the two contributions differ by a single-fermion exchange in the NMHV hexagon

$$\mathcal{W}^{(5)}_{7[1,1](1,1)}(\sigma',\sigma) = \mathcal{W}^{(4)}_{7[1,1](1,1)}(\sigma',\sigma) + \mathcal{W}_{6[1](1)}(\sigma')\,, \tag{31}$$

with

$$\mathcal{W}_{6[1](1)} = -i\int\limits_{\mathbb{R}+i0} d\mu_{\mathrm{F}}(u)x[u]\,. \tag{32}$$

It is the last term in the right-hand side of Eq. (31) that diverges when integrated with respect to σ'. This contribution gets subtracted in the Descent Equation (6) by the last term in its right-hand side.

3.2. Twist-two: fermion–gluon in final state

We now turn to twist-two effects. As exhibited by Eq. (21), at twist-two there is a contribution that enters with the helicity prefactor $\mathrm{e}^{3i\phi/2}$. It corresponds to a fermion–gluon pair absorbed by the top portion of the Wilson loop in a given OPE channel. Its all-order expression in coupling constant reads[5]

$$\begin{aligned}\mathcal{W}^{(j)}_{7[1,2](1,3)} = g\int\limits_{\mathbb{C}^+_\Psi} d\mu_\Psi(u_1)\int\limits_{\mathbb{C}^{(j)}_\Psi} d\mu_\Psi(v_1)\int\limits_{\mathbb{R}} d\mu_{\mathrm{g}}(v_2)\\ \times\frac{x[u_1]P_{\Psi|\mathrm{g}}(-u_1|v_2)P_{\Psi|\Psi}(-u_1|v_1)}{\sqrt{x^+[v_2]x^-[v_2]}P_{\mathrm{g}|\Psi}(v_2|v_1)P_{\mathrm{g}|\Psi}(-v_2|-v_1)}\,,\end{aligned} \tag{33}$$

where we used the factorized form of one-to-two particle transition pentagon [21] and fermion–gluon absorption form factor [20]. The helicity form factor is expressed in terms of the shifted Zhukowski variables $x^\pm[u] \equiv x[u^\pm]$ where $u^\pm = u \pm \frac{i}{2}$. The bottom fermion resides on the large sheet, while the one on the top can be split in the above formula into the small (f) and large (F) contributions

$$\mathcal{W}^{(j)}_{7[1,2](1,3)} = \mathcal{W}^{(j)}_{7\,\mathrm{F}|\mathrm{fg}} + \mathcal{W}^{(j)}_{7\,\mathrm{F}|\mathrm{Fg}}\,. \tag{34}$$

We start with the $j = 4$ case first. At lowest two orders in coupling, only the small fermion contributes to the Wilson loop and induces a nontrivial effect that reads

[5] All pentagon transitions used here and below can be found in Refs. [18,20,21].

$$\mathcal{W}^{(4)}_{7\,\mathrm{F|fg}} = g \int\limits_{\mathbb{R}+i0} d\mu_{\mathrm{F}}(u_1) x[u_1] \int\limits_{\mathbb{R}+i0} d\mu_{\mathrm{gf}}(v_2) \left[\frac{x^-[v_2]}{x^+[v_2]}\right]^{1/2} P_{\mathrm{F|g}}(-u_1|v_2) P_{\mathrm{F|f}}(-u_1|v_2^-)\,, \tag{35}$$

where we introduced the small-fermion–gluon measure [20],

$$\mu_{\mathrm{gf}}(v_2) = \operatorname*{res}_{v_1=v_2^-} \frac{g^2 \mu_{\mathrm{f}}(v_1)\mu_{\mathrm{g}}(v_2)}{x[v_1] P_{\mathrm{f|g}}(v_1|v_2) P_{\mathrm{f|g}}(-v_1|-v_2)}\,. \tag{36}$$

At $O(g^6)$ and higher, $\mathcal{W}_{7[1,2](1,3)}$ receives an additional term from the large fermion

$$\mathcal{W}^{(4)}_{7\,\mathrm{F|Fg}} = g \int\limits_{\mathbb{R}+i0} d\mu_{\mathrm{F}}(u_1) \int\limits_{\mathbb{R}+i0} d\mu_{\mathrm{F}}(v_1) \int\limits_{\mathbb{R}+i0} d\mu_{\mathrm{g}}(v_2) \times \frac{x[u_1] P_{\mathrm{F|g}}(-u_1|v_2) P_{\mathrm{F|F}}(-u_1|v_1)}{\sqrt{x^+[v_2]x^-[v_2]}\, P_{\mathrm{g|F}}(v_2|v_1) P_{\mathrm{g|F}}(-v_2|-v_1)}\,. \tag{37}$$

Similar analysis can be conducted for $j = 5$. The differences in the fermion contour result in differences of various contributions. The small fermion now reads instead

$$\mathcal{W}^{(5)}_{7\,\mathrm{F|fg}} = g \int\limits_{\mathbb{R}+i0} d\mu_{\mathrm{F}}(u_1) x[u_1] \int\limits_{\mathbb{R}} d\,\widetilde{\mu}_{\mathrm{gf}}(v_2) \left[\frac{x^+[v_2]}{x^-[v_2]}\right]^{1/2} P_{\mathrm{F|g}}(-u_1|v_2) P_{\mathrm{F|f}}(-u_1|v_2^+)\,, \tag{38}$$

where compared to the previous equation the composite measure has changed, since the pole $v_2 = v_1^+$ was picked up in the upper half plane of the lower Riemann sheet,

$$\widetilde{\mu}_{\mathrm{gf}}(v_2) = \operatorname*{res}_{v_1=v_2^+} \frac{g^2 \mu_{\mathrm{f}}(v_1)\mu_{\mathrm{g}}(v_2)}{x[v_1] P_{\mathrm{f|g}}(v_1|v_2) P_{\mathrm{f|g}}(-v_1|-v_2)}\,, \tag{39}$$

as well as the square root prefactor was flipped. As above, at order g^6 and beyond, the Wilson loop gets a new term from the large fermion. The expression for the latter is given by the same Eq. (37) except for the position of the contour in the v_1-fermion rapidity complex plane, i.e., one has to substitute $\int_{\mathbb{R}+i0} d\mu_{\mathrm{F}}(v_1) \to \int_{\mathbb{R}-i0} d\mu_{\mathrm{F}}(v_1)$. The correctness of these expressions can be verified by comparing them with the perturbative expansion of Ref. [29]. It would be important to extend this analysis to higher orders, especially in a fully analytic manner relying on the methods of Ref. [31], using the heptagon bootstrap program [32–35] that generalizes earlier results on the hexagon [36,37].

The calculation of the σ' integrals of contributions introduced in the previous section follows the same route as for the single fermion in Section 3.1, but now we have to evaluate the rapidity integral involving two pentagons. For the $j = 4$ contribution, this can be successfully accomplished order-by-order in perturbation theory and then resummed back into an exact function of 't Hooft coupling. For the integral involving the small and large fermions, $\Psi = \mathrm{f}, \mathrm{F}$, we find identical expressions for the right-hand side

$$\int du_1\, \mu_{\mathrm{F}}(u_1) \mathrm{e}^{-\tau'[E_{\mathrm{F}}(u_1)-1]} x[u_1] \delta\big(p_{\mathrm{F}}(u_1)\big) P_{\mathrm{F|}\Psi}(-u_1|v_2^-) P_{\mathrm{F|g}}(-u_1|v_2) = -\frac{2ig^3}{\Gamma(g)} \frac{1}{\sqrt{x^+[v_2]x^-[v_2]}}\,. \tag{40}$$

However, a simple counting of the powers of 't Hooft coupling for the large fermion demonstrates that its contribution gets postponed to one order higher than the integrand itself since the leading term in its perturbative expansion vanishes after the u_1 integration. Thus, the large fermion appears accompanied by a gluon starting only from three loops in the Descent Equation.

For $j = 5$, in complete analogy with the single fermion, the σ' integral turns out to be divergent. So it requires a subtraction. To make it as transparent as possible, let us calculate the difference between the χ_5 and χ_4 contributions first. A careful all-loop analysis demonstrates that the latter can be rewritten

$$\mathcal{W}^{(5)}_{7[1,2](1,3)} - \mathcal{W}^{(4)}_{7[1,2](1,3)} = \Delta\mathcal{W}_{7[1,2](1,3)} \tag{41}$$

in terms of the following expression

$$\Delta\mathcal{W}_{7[1,2](1,3)} \equiv \frac{1}{g}\int\limits_{\mathbb{R}+i0} d\mu_{\rm F}(u_1)\int\limits_{\mathbb{R}+i0} d\mu_{\rm g}(v_2)\, x[u_1]P_{\rm F|g}(-u_1|v_2)\sqrt{x^-[v_2]x^+[v_2]}\,. \tag{42}$$

It is important to emphasize that, starting from the three-loop order, the integrand of this equation does not develop u_1-dependence in addition to the one already present in the factor $x[u_1]\,\mu_{\rm F}[u_1]P_{\rm F|g}(-u_1|\dots)$ only when both the small $\Psi = {\rm f}$ and large $\Psi = {\rm F}$ fermions are accounted for in the twist-two state $|\Psi{\rm g}\rangle$!

To proceed further, we form the NMHV ratio functions,

$$\mathcal{P}^{(j)}_{7[1,2](1,3)}(\sigma',\sigma) = \mathcal{W}^{(j)}_{7[1,2](1,3)}(\sigma',\sigma) - \mathcal{W}^{(j)}_{7[1,1](1,1)}(\sigma',\sigma)\mathcal{W}_{6[1](2)}(\sigma)\,, \tag{43}$$

with the gluon flux-tube excitation propagating on the bosonic hexagon $\mathcal{W}_{6[1](2)}$, see Eq. (10). Substituting Eq. (31) into above (41), we find

$$\begin{aligned}&\mathcal{P}^{(5)}_{7[1,2](1,3)}(\sigma',\sigma)\\ &\quad= \mathcal{P}^{(4)}_{7[1,2](1,3)}(\sigma',\sigma) + \left[\Delta\mathcal{W}_{7[1,2](1,3)} - \mathcal{W}_{6[1](1)}(\sigma_1)\mathcal{W}_{6[1](2)}(\sigma)\right].\end{aligned} \tag{44}$$

The integral of the regularized expression is finite and can be cast in a concise form,

$$\begin{aligned}&\int d\sigma'\left[\Delta\mathcal{W}_{7[1,2](1,3)}(\sigma',\sigma) - \mathcal{W}_{6[1](1)}(\sigma')\mathcal{W}_{6[1](2)}(\sigma)\right]\\ &\quad= \frac{ig^2}{\Gamma(g)}\int\limits_{\mathbb{R}+i0} d\mu_{\rm g}(v_2)\left[x^-[v_2] - \frac{g^2}{x^+[v_2]} - \tfrac{i}{2}\left(E_{\rm g}(v_2) + ip_{\rm g}(v_2)\right)\right].\end{aligned} \tag{45}$$

This concludes our discussion of integrals involving fermion–gluon pairs in the OPE of the heptagon.

3.3. Twist-two: antifermion–scalar in final state

Finally, we address the $\mathcal{W}^{(j)}_{7[1,2](1,-1)}$. A simple counting of quantum numbers immediately suggests that there are two additive contributions, one from the hole–antifermion and another one from antigluon–fermion pair,

$$\mathcal{W}^{(j)}_{7[1,2](1,-1)} = \mathcal{W}^{(j)}_{7\,\Psi|\bar\Psi{\rm h}} + \mathcal{W}^{(j)}_{7\,\Psi|\Psi\bar{\rm g}}\,. \tag{46}$$

These admit a representation in terms of the pentagons as follows,

$$\mathcal{W}^{(j)}_{7\,\Psi|\bar\Psi\mathrm{h}} = \frac{2}{g^3}\int\limits_{\mathbb{C}_\Psi} d\mu_\Psi(u_1)\int\limits_{\mathbb{C}^{(j)}_\Psi} d\mu_\Psi(v_1)\int\limits_{\mathbb{R}} d\mu_{\mathrm{h}}(v_2)$$
$$\times\,\frac{x^{3/2}[u_1]x[v_1]P_{\Psi|\bar\Psi}(-u_1|v_1)P_{\Psi|\mathrm{h}}(-u_1|v_2)}{(v_1-v_2-\frac{i}{2})(v_1-v_2+\frac{3i}{2})P_{\Psi|\mathrm{h}}(v_1|v_2)P_{\Psi|\mathrm{h}}(-v_1|-v_2)}\,, \tag{47}$$

$$\mathcal{W}^{(j)}_{7\,\Psi|\Psi\bar{\mathrm{g}}} = g\int\limits_{\mathbb{C}_\Psi} d\mu_\Psi(u_1)\int\limits_{\mathbb{C}^{(j)}_\Psi} d\mu_\Psi(v_1)\int\limits_{\mathbb{R}+i0} d\mu_{\mathrm{g}}(v_2)$$
$$\times\,\frac{x[u_1]\sqrt{x^+[v_2]x^-[v_2]}P_{\Psi|\Psi}(-u_1|v_1)P_{\Psi|\bar{\mathrm{g}}}(-u_1|v_2)}{(v_1-v_2-\frac{i}{2})x[v_1]P_{\Psi|\bar{\mathrm{g}}}(v_1|v_2)P_{\Psi|\bar{\mathrm{g}}}(-v_1|-v_2)}\,. \tag{48}$$

Having these generic expressions, we can rewrite them in specific OPE channels accounting for the difference in the fermionic contours. For the $j=4$ channel, decomposing the fermion into the small and large contributions, we obtain

$$\mathcal{W}^{(4)}_{7[1,2](1,-1)} = \mathcal{W}^{(4)}_{7\,\mathrm{F}|\bar{\mathrm{f}}\mathrm{h}} + \mathcal{W}^{(4)}_{7\,\mathrm{F}|\bar{\mathrm{F}}\mathrm{h}} + \mathcal{W}^{(5)}_{7\,\mathrm{F}|\mathrm{F}\bar{\mathrm{g}}}\,. \tag{49}$$

The first term in the right-hand side starts at order g^2 and induces the tree-level term in the amplitude. The large antifermion–hole sets in an order higher, i.e., $O(g^4)$, while $\mathcal{W}^{(4)}_{7[1,2](1,-1)}$ starts receiving contributions from large-fermion–antigluon pair from two loops. They read individually,

$$\mathcal{W}^{(4)}_{7\,\mathrm{F}|\bar{\mathrm{f}}\mathrm{h}} = g\int\limits_{\mathbb{R}+i0} d\mu_{\mathrm{F}}(u_1)\int\limits_{\mathbb{R}} d\mu_{\mathrm{h}}(v_2)\mu_{\mathrm{f}}(v_2-\tfrac{3i}{2})$$
$$\times\,\frac{x^{3/2}[u_1]P_{\mathrm{F}|\bar{\mathrm{f}}}(-u_1|v_2-\frac{3i}{2})P_{\mathrm{F}|\mathrm{h}}(-u_1|v_2)}{x[v_2-\frac{3i}{2}]P_{\mathrm{f}|\mathrm{h}}(v_2-\frac{3i}{2}|v_2)P_{\mathrm{f}|\mathrm{h}}(-v_2+\frac{3i}{2}|-v_2)}\,, \tag{50}$$

$$\mathcal{W}^{(4)}_{7\,\mathrm{F}|\bar{\mathrm{F}}\mathrm{h}} = \frac{2}{g^3}\int\limits_{\mathbb{R}+i0} d\mu_{\mathrm{F}}(u_1)\int\limits_{\mathbb{R}+i0} d\mu_{\mathrm{F}}(v_1)\int\limits_{\mathbb{R}} d\mu_{\mathrm{h}}(v_2)$$
$$\times\,\frac{x^{3/2}[u_1]x[v_1]P_{\mathrm{F}|\bar{\mathrm{F}}}(-u_1|v_1)P_{\mathrm{F}|\mathrm{h}}(-u_1|v_2)}{(v_1-v_2-\frac{i}{2})(v_1-v_2+\frac{3i}{2})P_{\mathrm{F}|\mathrm{h}}(v_1|v_2)P_{\mathrm{F}|\mathrm{h}}(-v_1|-v_2)}\,, \tag{51}$$

$$\mathcal{W}^{(4)}_{7\,\mathrm{F}|\mathrm{F}\bar{\mathrm{g}}} = g\int\limits_{\mathbb{R}+i0} d\mu_{\mathrm{F}}(u_1)\int\limits_{\mathbb{R}+i0} d\mu_{\mathrm{F}}(v_1)\int\limits_{\mathbb{R}+i0} d\mu_{\mathrm{g}}(v_2)$$
$$\times\,\frac{x[u_1]\sqrt{x^+[v_2]x^-[v_2]}P_{\mathrm{F}|\mathrm{F}}(-u_1|v_1)P_{\mathrm{F}|\bar{\mathrm{g}}}(-u_1|v_2)}{(v_1-v_2-\frac{i}{2})x[v_1]P_{\mathrm{F}|\bar{\mathrm{g}}}(v_1|v_2)P_{\mathrm{F}|\bar{\mathrm{g}}}(-v_1|-v_2)}\,. \tag{52}$$

For the $\chi_1^3\chi_5$ channel, all one has to do is to use the corresponding fermion contour. Then one immediately realizes that compared to the previously studied sector, there will be an additional contribution from the small-fermion–antigluon in Eq. (48) due to the location of the simple pole above the real axis where we close our integration contour. Then we have

$$\mathcal{W}^{(5)}_{7[1,2](1,-1)} = \mathcal{W}^{(5)}_{7\,\mathrm{F}|\bar{\mathrm{f}}\mathrm{h}} + \mathcal{W}^{(5)}_{7\,\mathrm{F}|\bar{\mathrm{F}}\mathrm{h}} + \mathcal{W}^{(5)}_{7\,\mathrm{F}|\bar{\mathrm{f}}\bar{\mathrm{g}}} + \mathcal{W}^{(5)}_{7\,\mathrm{F}|\mathrm{F}\bar{\mathrm{g}}}\,. \tag{53}$$

To the lowest two orders of perturbation theory only small fermions contribute to the right-hand side as we now explain. Namely, closing the integration contour in the upper half plane in $\mathcal{W}_{\Psi|\bar\Psi h}$ yields the result for the $\mathcal{W}^{(5)}_{7\,\mathrm{F}|\bar{\mathrm{f}}\mathrm{h}}$,

$$\mathcal{W}^{(5)}_{7\mathrm{F}|\bar{\mathrm{f}}\mathrm{h}} = g\int\limits_{\mathbb{R}+i0} d\mu_{\mathrm{F}}(u_1)\int\limits_{\mathbb{R}} d\mu_{\mathrm{h}}(v_2)\mu_{\mathrm{f}}(v_2^+)\frac{x^{3/2}[u_1]P_{\mathrm{F}|\bar{\mathrm{f}}}(-u_1|v_2^+)P_{\mathrm{F}|\mathrm{h}}(-u_1|v_2)}{x^+[v_2]P_{\mathrm{f}|\mathrm{h}}(v_2^+|v_2)P_{\mathrm{f}|\mathrm{h}}(-v_2^+|-v_2)}\,. \tag{54}$$

The large-fermion case is determined by the integrand of Eq. (51) with the v_2 integral running just below the real axis, $\mathbb{R}-i0$. This contribution vanishes at $O(g^4)$. At this order the small fermion in the pair with antigluon

$$\mathcal{W}^{(5)}_{7\,\mathrm{F}|\mathrm{f}\bar{\mathrm{g}}} = \frac{1}{g}\int\limits_{\mathbb{R}+i0} d\mu_{\mathrm{F}}(u_1)x[u_1]\int\limits_{\mathbb{R}} d\mu_{\mathrm{g}}(v_2)\mu_{\mathrm{f}}(v_2^+)x^+[v_2]\sqrt{x^+[v_2]x^-[v_2]}$$
$$\times\frac{P_{\mathrm{F}|\mathrm{f}}(-u_1|v_2^+)P_{\mathrm{F}|\bar{\mathrm{g}}}(-u_1|v_2)}{P_{\mathrm{f}|\bar{\mathrm{g}}}(v_2^+|v_2)P_{\mathrm{f}|\bar{\mathrm{g}}}(-v_2^+|-v_2)} \tag{55}$$

starts at one loop, postponing the effect of the large fermion to two loops. The latter is determined by the same equation as in (52), where one has to shift the integration contour with respect to v_2 in the lower half-plane. Expansion in 't Hooft coupling allows us to support these predictions at lowest two orders by confronting them with explicit amplitudes [29].

To uncover contributions of the above twist-two effects in the Descent Equation, we have to finally evaluate the σ' integrals. Again we start with the convergent $j=4$ operator channel. To this end, we need the following set of rapidity integrals involving the antifermion and the hole,

$$\int du_1\,\mu_{\mathrm{F}}(u_1)\mathrm{e}^{-\tau'[E_{\mathrm{F}}(u_1)-1]}x[u_1]\delta\big(p_{\mathrm{F}}(u_1)\big)P_{\mathrm{F}|\bar\Psi}(-u_1|v_1)P_{\mathrm{F}|\mathrm{h}}(-u_1|v_2) = \frac{2g^3}{\Gamma(g)}\,. \tag{56}$$

This equation is the same for both the small $\bar\Psi=\bar{\mathrm{f}}$ and large $\bar\Psi=\bar{\mathrm{F}}$ antifermion except that one has to set its rapidity to $v_1=v_2-\frac{3i}{2}$ in the former case. Last but not least, for the large fermion and antigluon we find

$$\int du_1\,\mu_{\mathrm{F}}(u_1)\mathrm{e}^{-\tau'[E_{\mathrm{F}}(u_1)-1]}x[u_1]\delta\big(p_{\mathrm{F}}(u_1)\big)P_{\mathrm{F}|\mathrm{F}}(-u_1|v_1)P_{\mathrm{F}|\bar{\mathrm{g}}}(-u_1|v_2)$$
$$= -\frac{2g}{\Gamma(g)}\sqrt{x^+[v_2]x^-[v_2]}\,. \tag{57}$$

Now we move to the $j=5$ case. First, for antifermion–hole contribution $\mathcal{W}^{(5)}_{7\,\Psi|\bar\Psi\mathrm{h}}$, we find that the integral involving the small antifermion is identical to Eq. (56). In fact, these two are particular cases of a more general formula for a generic value of v_1 in $P_{\mathrm{F}|\bar{\mathrm{f}}}(-u_1|v_1)$. Next, for the large fermion we can use Eq. (56) in spite of the fact that the integration contour for the outgoing fermion lies below the real axis. The reason for this is that while crossing the real axis one acquires a pole along the way, this term is not singular for $u_1=0$. Finally, we turn to the antigluon–fermion final state, $\mathcal{W}^{(5)}_{7\,\Psi|\Psi\bar{\mathrm{g}}}$. In this case, the σ' integral is not convergent, so one has to form the ratio function and thus subtract a factorized contribution,

$$\mathcal{P}^{(5)}_{7[1,2](1,-1)}(\sigma',\sigma) = \mathcal{W}^{(5)}_{7[1,2](1,-1)}(\sigma',\sigma) - \mathcal{W}^{(5)}_{7[1,1](1,1)}(\sigma',\sigma)\mathcal{W}_{6[1](2)}(\sigma)\,. \tag{58}$$

Substituting (31), we can split the result into two terms,

$$\begin{aligned}
&\mathcal{W}^{(5)}_{7\,\Psi|\Psi\bar{\mathrm{g}}}(\sigma',\sigma)-\mathcal{W}^{(5)}_{7[1,1](1,1)}(\sigma',\sigma)\mathcal{W}_{6[1](2)}(\sigma)\\
&\quad=\mathcal{W}^{(4)}_{7\,\Psi|\Psi\bar{\mathrm{g}}}(\sigma',\sigma)-\mathcal{W}^{(4)}_{7[1,1](1,1)}(\sigma',\sigma)\mathcal{W}_{6[1](2)}(\sigma)\\
&\qquad+\left[\Delta\mathcal{W}^{(5)}_{7\,\Psi|\Psi\bar{\mathrm{g}}}(\sigma',\sigma)-\mathcal{W}_{6[1](1)}(\sigma')\mathcal{W}_{6[1](2)}(\sigma)\right],
\end{aligned}\tag{59}$$

with the first two terms in its right-hand side addressed in the previous sections. The integral of the square bracket can be expressed in a concise form

$$\begin{aligned}
&\int_0^\infty d\sigma'\left[\Delta\mathcal{W}^{(5)}_{7\,\Psi|\Psi\bar{\mathrm{g}}}(\sigma',\sigma)-\mathcal{W}_{6[1](1)}(\sigma')\mathcal{W}_{6[1](2)}(\sigma)\right]\\
&\quad=\frac{ig^2}{\Gamma(g)}\int d\mu_{\mathrm{g}}(v_2)\left[-x^-[v_2]+\frac{g^2}{x^+[v_2]}-\tfrac{i}{2}\left(E_{\mathrm{g}}(v_2)+ip_{\mathrm{g}}(v_2)\right)\right].
\end{aligned}\tag{60}$$

This concludes our OPE analysis.

4. Verifying the conjecture

One can now combine all of the above ingredients together and substitute them into the Descent Equation. We will not give the cumulative formula here to save space. It is obvious from the representation of these results, that the overall power of the inverse cusp anomalous dimension cancels against the one in the right-hand side of Eq. (6). Thus, this proves the all-order form of the Descent Equation provided that we can establish the agreement between OPE series on both of its sides.

As we discussed earlier, the $O(g^4)$ contribution is in agreement with the last term in Eq. (13) as can now be confirmed making use of the explicit results derived in the previous section. However, it is important to realize that staying at this order is not sufficient to unambiguously constrain the form of the conjectured expression for the cyclic shift. Namely, there is an empirically found relation between $\mathcal{W}^{(4)}_{7[1,2](1,-1)}$ and $\mathcal{W}^{(4)}_{7[1,2](1,3)}$ components of the superloop,

$$\mathcal{W}^{(4)}_{7[1,2](1,-1)}=\mathcal{W}^{(4)}_{7[1,2](1,3)}+\mathrm{e}^{\sigma}\mathcal{W}^{(4)}_{7[1,1](1,1)}+O(g^6),\tag{61}$$

which is valid to order g^4 only. Thus, without further checks, there are two possible forms for the right hand side of Eq. (23): the one that is quoted out there and another one that one obtains by eliminating, say, $\mathcal{W}^{(4)}_{7[1,2](1,-1)}$ via Eq. (61) from it. The latter implies that one can replace $\mathcal{P}^{(4)}_{7\,[1,2](1,-1)}+\mathcal{P}^{(4)}_{7\,[1,2](1,3)}+\mathrm{e}^{\sigma}\mathcal{P}^{(4)}_{7\,[1,1](1,1)}\to 2\mathcal{P}^{(4)}_{7\,[1,2](1,-1)}$ in Eq. (23). Thus the left-hand side of Eq. (23) does not appear to be unique. However, higher order corrections to two-particle contributions eventually lift the degeneracy between the two seemingly equivalent representations and allow us to pick just one. In addition, the inconsistency of the relation (61) with the anticipated OPE representation for the $\mathcal{P}^{(4)}_{7\,[1,2](1,-1)}$ can be observed even without pushing the program beyond the lowest two perturbative orders in (54). Namely, the pole at $v_2=v_1^+$ is not at the right side of the real axis to be naturally accommodated into OPE. There is an immediate problem that one needs to reconcile, namely, how the two results, Eq. (54) and (49) can be compatible. The first one has only small fermion contribution while the latter one has both, large and small. It turns out that if one ignores the proper choice of the contour and uses $\mathbb{C}^-_\Psi$ instead of $\mathbb{C}^+_\Psi$, then $\mathbb{C}^+_{\mathrm{f}}$ is closed in the upper half plane and one picks up a pole at $v_2=v_1^+$ and gets the result given in Eq. (54). At the same time, as we already mentioned before, the genuine two-particle twist-two

contribution (that sets in at order g^4) vanishes, so one is left with small-fermion–hole pair alone as found in the relation (61).

Therefore, to put the result (23) on a firmer foundation, we compared the left- and right-hand sides of the Descent Equation at $O(g^6)$, when all two-particle excitations contribute to the OPE. As a result, we confirmed the agreement, i.e., the equality of Eq. (12) to the sum of Eq. (15) and (24) multiplied by the factor of the cusp anomalous dimension. This is the main result of this paper.

5. Conclusions

In this work, we analyzed the Descent Equation for the null polygonal superWilson loop within the framework of the pentagon OPE. We demonstrated that the factor of the cusp anomalous dimensions naturally arises in its right-hand side from the pentagon formalism confirming in this manner the all-loop structure of the equation. We have established a phenomenon of twist enhancement as one passes to an adjacent channel by cyclicity. Namely, the leading effect comes from the subleading-twist contributions of the direct channel. When added up with the twist-one excitations in the direct channel, it proves the consistency of the OPE expansion with the $\bar{Q}$-equation. It would be interesting to extend this consideration to event higher twists and other nonMHV polygons.

It is important to derive our conjecture, and more generally confirm the twist enhancement phenomenon, from the physics of flux-tube excitations. Hopefully, there is a map that allows one to go between cyclic channels by performing a suitable analytic continuation in the complex rapidity plane. There are two, available to date, examples of twist increase in different contexts. One arises in the attempt to find a mirror transformation for the flux-tube fermion [17] and another one for the octet reggeons starting from flux-tube gluons [38].

Finally, it would be interesting to verify the consistency of various relations arising in the current analysis, like Eqs. (40), (56) etc., at strong coupling, see, e.g., Refs. [39,40]. These questions will be addressed in a future publication.

Acknowledgements

We would like to thank Jacob Bourjaily for very instructive correspondence and the organizers of the "Flux-tube Workshop" for hospitality at Perimeter Institute at the final stages of this work. This research was supported by the U.S. National Science Foundation under the grants PHY-1068286 and PHY-1403891.

Appendix A. Parametrization of polygons

Making use of the projective invariance of momentum twistors, we will use the following rescaled version of the later for the hexagon

$$
\begin{aligned}
Z_1^{(6)} &= \left(\mathrm{e}^{-\tau+2\sigma}, 0, \mathrm{e}^{\sigma+i\phi}, \mathrm{e}^{-2\tau+\sigma+i\phi}\right) , \\
Z_2^{(6)} &= (1,0,0,0) , \\
Z_3^{(6)} &= (-1,0,0,1) , \\
Z_4^{(6)} &= (0,1,-1,1) ,
\end{aligned}
$$

$$
\begin{aligned}
Z_5^{(6)} &= (0,1,0,0)\,,\\
Z_6^{(6)} &= \left(0,\mathrm{e}^{-\tau},\mathrm{e}^{\sigma+i\phi},0\right),
\end{aligned}
\tag{62}
$$

and heptagon

$$
\begin{aligned}
Z_1^{(7)} &= \left(\mathrm{e}^{-\tau'+2\sigma'},0,\mathrm{e}^{\sigma'+i\phi'},\mathrm{e}^{-2\tau'+\sigma'+i\phi'}\right),\\
Z_2^{(7)} &= (1,0,0,0)\,,\\
Z_3^{(7)} &= (-1,0,0,1)\,,\\
Z_4^{(7)} &= \left(-\mathrm{e}^{-\tau},\mathrm{e}^{-\sigma-i\phi},-\mathrm{e}^{-\sigma-i\phi},\mathrm{e}^{-\sigma-i\phi}(1+\mathrm{e}^{-2\tau})+\mathrm{e}^{-\tau}\right),\\
Z_5^{(7)} &= \left(0,\mathrm{e}^{-\sigma-i\phi}+\mathrm{e}^{-\tau-2\sigma},-\mathrm{e}^{-\sigma-i\phi},\mathrm{e}^{-\sigma-i\phi}\right),\\
Z_6^{(7)} &= (0,1,0,0)\,,\\
Z_7^{(7)} &= \left(0,\mathrm{e}^{-\tau'},\mathrm{e}^{\sigma'+i\phi'},0\right),
\end{aligned}
\tag{63}
$$

respectively, compared to Refs. [16,21]. These are very well suited for the collinear expansion within the framework of the Descent Equation, in particular ensuring Eq. (7).

The collinear limit $Z_1 \to Z_7$ at the bottom of the heptagon leaves just three conformal cross ratios analogous to the one of the hexagon and one non-spacetime cross ratio

$$
\begin{aligned}
w_1 &= \frac{(2,3,4,5)(5,6,7,2)}{(2,3,5,6)(4,5,7,2)}\bigg|_{\tau'\to\infty} = \frac{\mathrm{e}^{i\phi}}{\mathrm{e}^{2\sigma+i\phi}+\mathrm{e}^{-\tau+\sigma}+\mathrm{e}^{-\tau+\sigma+2i\phi}+\mathrm{e}^{i\phi}(1+\mathrm{e}^{-2\tau})}\,,\\
w_2 &= \frac{(3,4,5,6)(6,7,2,3)}{(3,4,6,7)(2,3,5,6)}\bigg|_{\tau'\to\infty} = \frac{\mathrm{e}^{-2\tau}}{1+\mathrm{e}^{-2\tau}}\,,\\
w_3 &= \frac{(4,5,6,7)(7,2,3,4)}{(4,5,7,2)(3,4,6,7)}\bigg|_{\tau'\to\infty} = \frac{\mathrm{e}^{2\sigma}}{1+\mathrm{e}^{-2\tau}}w_1\,,\\
w &= \frac{(6,7,3,5)(7,2,3,4)}{(6,7,3,4)(7,2,3,5)}\bigg|_{\tau'\to\infty} = \frac{\mathrm{e}^{\sigma}}{(1+\mathrm{e}^{-2\tau})(\mathrm{e}^{\sigma}+\mathrm{e}^{-\tau+i\phi})}\,.
\end{aligned}
$$

We also introduce cyclically shifted cross ratios $i \to i+1$,

$$
\begin{aligned}
\tilde{w}_1 &= \frac{(3,4,5,6)(6,7,2,3)}{(3,4,6,7)(5,6,2,3)}\bigg|_{\tau'\to\infty} = w_2\,,\\
\tilde{w}_2 &= \frac{(4,5,6,7)(7,2,3,4)}{(4,5,7,2)(3,4,6,7)}\bigg|_{\tau'\to\infty} = w_3\,,\\
\tilde{w}_3 &= \frac{(5,6,7,2)(2,3,4,5)}{(5,6,2,3)(4,5,7,2)}\bigg|_{\tau'\to\infty} = w_1\,,\\
\tilde{w} &= \frac{(7,2,4,6)(2,3,4,5)}{(7,2,4,5)(2,3,4,6)}\bigg|_{\tau'\to\infty} = \left(1+\mathrm{e}^{-\tau+\sigma+i\phi}+\mathrm{e}^{-2\tau}\right)w_1\,.
\end{aligned}
\tag{64}
$$

The latter will be relevant for establishing the form of the cyclic permutation form of the χ_5 contribution to the one-loop heptagon.

References

[1] L.F. Alday, J.M. Maldacena, Gluon scattering amplitudes at strong coupling, J. High Energy Phys. 0706 (2007) 064, arXiv:0705.0303 [hep-th].
[2] J.M. Drummond, J. Henn, G.P. Korchemsky, E. Sokatchev, On planar gluon amplitudes/Wilson loops duality, Nucl. Phys. B 795 (2008) 52, arXiv:0709.2368 [hep-th].
[3] A. Brandhuber, P. Heslop, G. Travaglini, MHV amplitudes in $N = 4$ super Yang–Mills and Wilson loops, Nucl. Phys. B 794 (2008) 231, arXiv:0707.1153 [hep-th].
[4] S. Caron-Huot, Notes on the scattering amplitude/Wilson loop duality, J. High Energy Phys. 1107 (2011) 058, arXiv:1010.1167 [hep-th].
[5] L.J. Mason, D. Skinner, The complete planar S-matrix of $N = 4$ SYM as a Wilson loop in twistor space, J. High Energy Phys. 1012 (2010) 018, arXiv:1009.2225 [hep-th].
[6] A.V. Belitsky, G.P. Korchemsky, E. Sokatchev, Are scattering amplitudes dual to super Wilson loops?, Nucl. Phys. B 855 (2012) 333, arXiv:1103.3008 [hep-th].
[7] L.F. Alday, D. Gaiotto, J. Maldacena, A. Sever, P. Vieira, An operator product expansion for polygonal null Wilson loops, J. High Energy Phys. 1104 (2011) 088, arXiv:1006.2788 [hep-th].
[8] D. Gaiotto, J. Maldacena, A. Sever, P. Vieira, Pulling the straps of polygons, J. High Energy Phys. 1112 (2011) 011, arXiv:1102.0062 [hep-th].
[9] A.V. Belitsky, OPE for null Wilson loops and open spin chains, Phys. Lett. B 709 (2012) 280, arXiv:1110.1063 [hep-th].
[10] A. Sever, P. Vieira, T. Wang, From polygon Wilson loops to spin chains and back, J. High Energy Phys. 1212 (2012) 065, arXiv:1208.0841 [hep-th].
[11] B. Basso, A. Sever, P. Vieira, Spacetime and flux tube S-matrices at finite coupling for $N = 4$ supersymmetric Yang–Mills theory, Phys. Rev. Lett. 111 (9) (2013) 091602, arXiv:1303.1396 [hep-th].
[12] B. Basso, Exciting the GKP string at any coupling, Nucl. Phys. B 857 (2012) 254, arXiv:1010.5237 [hep-th].
[13] B. Basso, A.V. Belitsky, Lüscher formula for GKP string, Nucl. Phys. B 860 (2012) 1, arXiv:1108.0999 [hep-th].
[14] D. Fioravanti, S. Piscaglia, M. Rossi, On the scattering over the GKP vacuum, Phys. Lett. B 728 (2014) 288, arXiv:1306.2292 [hep-th].
[15] B. Basso, A. Rej, Bethe ansätze for GKP strings, Nucl. Phys. B 879 (2014) 162, arXiv:1306.1741 [hep-th].
[16] B. Basso, A. Sever, P. Vieira, Space–time S-matrix and flux tube S-matrix II. Extracting and matching data, J. High Energy Phys. 1401 (2014) 008, arXiv:1306.2058 [hep-th].
[17] B. Basso, A. Sever, P. Vieira, Space–time S-matrix and flux-tube S-matrix III. The two-particle contributions, J. High Energy Phys. 1408 (2014) 085, arXiv:1402.3307 [hep-th].
[18] A.V. Belitsky, Nonsinglet pentagons and NHMV amplitudes, Nucl. Phys. B 896 (2015) 493, arXiv:1407.2853 [hep-th].
[19] B. Basso, A. Sever, P. Vieira, Space–time S-matrix and flux-tube S-matrix IV. Gluons and fusion, J. High Energy Phys. 1409 (2014) 149, arXiv:1407.1736 [hep-th].
[20] A.V. Belitsky, Fermionic pentagons and NMHV hexagon, Nucl. Phys. B 894 (2015) 108, arXiv:1410.2534 [hep-th].
[21] A.V. Belitsky, On factorization of multiparticle pentagons, Nucl. Phys. B 897 (2015) 346, arXiv:1501.06860 [hep-th].
[22] B. Basso, J. Caetano, L. Cordova, A. Sever, P. Vieira, OPE for all helicity amplitudes, arXiv:1412.1132 [hep-th].
[23] J.M. Drummond, J. Henn, G.P. Korchemsky, E. Sokatchev, Dual superconformal symmetry of scattering amplitudes in $N = 4$ super-Yang–Mills theory, Nucl. Phys. B 828 (2010) 317, arXiv:0807.1095 [hep-th].
[24] L.J. Mason, D. Skinner, Dual superconformal invariance, momentum twistors and Grassmannians, J. High Energy Phys. 0911 (2009) 045, arXiv:0909.0250 [hep-th].
[25] N. Arkani-Hamed, J. Trnka, The amplituhedron, J. High Energy Phys. 1410 (2014) 30, arXiv:1312.2007 [hep-th]; N. Arkani-Hamed, J. Trnka, Into the amplituhedron, J. High Energy Phys. 1412 (2014) 182, arXiv:1312.7878 [hep-th].
[26] S. Caron-Huot, S. He, Jumpstarting the all-loop S-matrix of planar $N = 4$ Super Yang–Mills, J. High Energy Phys. 1207 (2012) 174, arXiv:1112.1060 [hep-th].
[27] M. Bullimore, D. Skinner, Descent Equations for superamplitudes, arXiv:1112.1056 [hep-th].
[28] A. Hodges, Eliminating spurious poles from gauge-theoretic amplitudes, J. High Energy Phys. 1305 (2013) 135, arXiv:0905.1473 [hep-th].
[29] J.L. Bourjaily, S. Caron-Huot, J. Trnka, Dual-conformal regularization of infrared loop divergences and the chiral box expansion, J. High Energy Phys. 1501 (2015) 001, arXiv:1303.4734 [hep-th].

[30] L.F. Alday, J.M. Maldacena, Comments on operators with large spin, J. High Energy Phys. 0711 (2007) 019, arXiv:0708.0672 [hep-th].
[31] G. Papathanasiou, Hexagon Wilson loop OPE and harmonic polylogarithms, J. High Energy Phys. 1311 (2013) 150, arXiv:1310.5735 [hep-th].
[32] J. Golden, M.F. Paulos, M. Spradlin, A. Volovich, Cluster polylogarithms for scattering amplitudes, J. Phys. A 47 (2014) 47, 474005, arXiv:1401.6446 [hep-th].
[33] J. Golden, M. Spradlin, An analytic result for the two-loop seven-point MHV amplitude in $\mathcal{N} = 4$ SYM, J. High Energy Phys. 1408 (2014) 154, arXiv:1406.2055 [hep-th].
[34] J. Golden, M. Spradlin, A cluster bootstrap for two-loop MHV amplitudes, J. High Energy Phys. 1502 (2015) 002, arXiv:1411.3289 [hep-th].
[35] J.M. Drummond, G. Papathanasiou, M. Spradlin, A symbol of uniqueness: the cluster bootstrap for the 3-loop MHV heptagon, J. High Energy Phys. 1503 (2015) 072, arXiv:1412.3763 [hep-th].
[36] L.J. Dixon, J.M. Drummond, J.M. Henn, Analytic result for the two-loop six-point NMHV amplitude in $N = 4$ super Yang–Mills theory, J. High Energy Phys. 1201 (2012) 024, arXiv:1111.1704 [hep-th].
[37] L.J. Dixon, M. von Hippel, Bootstrapping an NMHV amplitude through three loops, J. High Energy Phys. 1410 (2014) 65, arXiv:1408.1505 [hep-th].
[38] B. Basso, S. Caron-Huot, A. Sever, Adjoint BFKL at finite coupling: a short-cut from the collinear limit, J. High Energy Phys. 1501 (2015) 027, arXiv:1407.3766 [hep-th].
[39] B. Basso, A. Sever, P. Vieira, Collinear limit of scattering amplitudes at strong coupling, Phys. Rev. Lett. 113 (26) (2014) 261604, arXiv:1405.6350 [hep-th].
[40] D. Fioravanti, S. Piscaglia, M. Rossi, Asymptotic Bethe Ansatz on the GKP vacuum as a defect spin chain: scattering, particles and minimal area Wilson loops, arXiv:1503.08795 [hep-th].